

# Bridging the size gap between density-functional and many-body perturbation theory

P. Umari,<sup>1</sup> Geoffrey Stenuit,<sup>1</sup> and Stefano Baroni<sup>2,1</sup>

<sup>1</sup> INFM-CNR DEMOCRITOS Theory@Elettra group,

c/o Sincrotrone Trieste, Area Science Park, I-34012 Basovizza, Trieste, Italy

<sup>2</sup> SISSA – Scuola Internazionale Superiore di Studi Avanzati, via Beirut 2-4, I-34014 Trieste Grignano, Italy

(Dated: November 10, 2008)

The calculation of quasi-particle spectra based on the GW approximation is extended to systems of hundreds of atoms, thus expanding the size range of current approaches by more than one order of magnitude. This is achieved through an optimal strategy, based on the use of Wannier-like orbitals, for evaluating the polarization propagator. Our method is validated by calculating the vertical ionization energies of the benzene molecule and the band structure of crystalline silicon. Its potentials are then demonstrated by addressing the quasi-particle spectrum of a model structure of vitreous silica, as well as of the tetraphenylporphyrin molecule.

PACS numbers: 31.15.xm 71.15.Qe 77.22.-d,

Density-functional theory (DFT) has grown into a powerful tool for the numerical simulation of matter at the nanoscale, allowing one to study the structure and dynamics of realistic models of materials consisting of up to a few thousands atoms, these days [1]. The scope of standard DFT, however, is limited to those dynamical processes that do not involve electronic excitations. The most elementary such excitation is the removal/addition of an electron from a system originally in its ground state. These processes are accessible to direct/inverse photo-emission spectroscopies and can be described in terms of *quasi-particle* (QP) spectra [2]. In insulators, the energy difference between the lowest-lying quasi-electron state and the highest-lying quasi-hole state is the QP band gap, a quantity that is severely (and to some extent erratically) underestimated by DFT [3].

Many-body perturbation theory (MBPT), in turn, provides a general, though unwieldy, framework for QP and other excitation (such as optical) spectra [2]. A numerically viable approach to QP energy levels (known as the GW approximation, GWA) was introduced in the 60's [4], but it took two decades for a realistic application of it to appear [5], and even today the numerical effort required by MBPT is such that its scope is limited to systems of a few handfuls of atoms. Even so, and in spite of the success met by MBPT in real materials [6], the approximations made for the most demanding of its applications are such as to shed some legitimate doubts on their general applicability. This situation will be referred to as the *size gap* of MBPT calculations.

In this letter we present a strategy to substantially reduce the size gap of MBPT, based on the adoption of Wannier-like orbitals [7, 8, 9] to represent the response functions whose calculation is the main size-limiting factor of MBPT. Although we focus on QP spectra within the GWA, this strategy easily generalizes to optical spectra, as calculated from the Bethe-Salpeter equation [10]. Our method is benchmarked by the calculation of the ionization potentials of the benzene molecule and of

the band structure of crystalline silicon, and its potentials demonstrated by case calculations on vitreous silica and on the free-base tetraphenylporphyrin molecule (TPPH<sub>2</sub>).

QP energies (QPE) are eigenvalues of a Schrödinger-like equation (QPEq) for the so-called QP amplitudes (QPA), which is similar to the DFT Kohn-Sham equation with the exchange-correlation potential,  $V_{xc}(\mathbf{r})$ , replaced by the non-local, energy-dependent, and non-Hermitian self-energy operator,  $\tilde{\Sigma}(\mathbf{r}, \mathbf{r}', E)$  (a tilde indicates the Fourier transform of a time-dependent function). Setting  $\tilde{\Sigma}(\mathbf{r}, \mathbf{r}'; E) = -\frac{\rho(\mathbf{r}, \mathbf{r}')}{|\mathbf{r} - \mathbf{r}'|}$  ( $\rho$  being the one-particle density matrix) would turn the QPEq into the Hartree-Fock equation. The next level of approximation is the GWA [4] where  $\tilde{\Sigma}$  is the product of the one-electron propagator,  $G$ , and of the dynamically screened interaction,  $W$ :

$$\Sigma_{GW}(\mathbf{r}, \mathbf{r}'; t - t') = iG(\mathbf{r}, \mathbf{r}'; t - t')W(\mathbf{r}, \mathbf{r}'; t - t'), \quad (1)$$

where  $W = v + v \cdot \Pi \cdot v$ ,  $\Pi(\mathbf{r}, \mathbf{r}'; t - t') = \frac{\delta n(\mathbf{r}, t)}{\delta V(\mathbf{r}', t')} = (1 - P \cdot v)^{-1} \cdot P$  is the reducible electron polarization propagator (polarizability),  $P$  its irreducible counterpart,  $v(\mathbf{r}, \mathbf{r}'; t - t') = \frac{1}{|\mathbf{r} - \mathbf{r}'|} \delta(t - t')$  is the bare Coulomb interaction,  $n$  and  $V$  are the electron density distribution and external potential, respectively, and a dot indicates the product of two operators, such as in  $v \cdot \chi(\mathbf{r}, \mathbf{r}', t - t') = \int d\mathbf{r}'' dt'' v(\mathbf{r}, \mathbf{r}''; t - t'') \chi(\mathbf{r}'', \mathbf{r}'; t'' - t')$ .

The GWA alone does not permit to solve the QPEq, unless  $G$  and  $W$  are known, possibly depending on the solution of the QPEq itself. One of the most popular further approximations is the so called  $G^{\circ}W^{\circ}$  approximation ( $G^{\circ}W^{\circ}A$ ), where the one-electron propagator is obtained from the QPEq using a model real and energy-independent self-energy, such as *e.g.*  $\tilde{\Sigma}^{\circ} = V_{xc}(\mathbf{r})\delta(\mathbf{r} - \mathbf{r}')$ , and the irreducible polarizability is calculated in the random-phase approximation (RPA):  $G^{\circ}(\mathbf{r}, \mathbf{r}'; \tau) = i \sum_v \psi_v(\mathbf{r})\psi_v^*(\mathbf{r}')e^{-i\epsilon_v \tau} \theta(-\tau) - i \sum_c \psi_c(\mathbf{r})\psi_c^*(\mathbf{r}')e^{-i\epsilon_c \tau} \theta(\tau)$  ( $\psi$  and  $\epsilon$  are zero-th order QPAs and QPEs, referred to the Fermi energy,  $v$  and

$c$  suffixes indicate states below and above the Fermi energy, respectively, and  $\theta$  is the Heaviside step function) and  $P^\circ(\mathbf{r}, \mathbf{r}'; \tau) = -iG^\circ(\mathbf{r}, \mathbf{r}'; \tau)G^\circ(\mathbf{r}', \mathbf{r}; -\tau)$ . To first order in  $\Sigma' = \Sigma_{G^\circ W^\circ} - \Sigma^\circ$ , QPEs are given by the equation:

$$E_n \approx \epsilon_n + \langle \tilde{\Sigma}_{G^\circ W^\circ}(E_n) \rangle_n - \langle V_{XC} \rangle_n, \quad (2)$$

where  $\langle A \rangle_n = \langle \psi_n | A | \psi_n \rangle$ .

The apparently simple  $G^\circ W^\circ A$  still involves severe difficulties, mainly related to the calculation and manipulation of the polarizability that enters the definition of  $W^\circ$ . These difficulties are often addressed using the so called plasmon-pole approximation [5], which however introduces noticeable ambiguities and inaccuracies when applied to inhomogeneous systems [11]. A well established technique to address QP spectra in real materials without any crude approximations on response functions is the *space-time method* (STM) by Godby *et al.* [12]. In the STM the time/energy dependence of the  $G^\circ W^\circ$  operators is represented on the imaginary axis, thus making them smooth (in the frequency domain) or exponentially decaying (in the time domain). The various operators are represented on a real-space grid, a choice which is straightforward, but impractical for systems larger than a few handfuls of inequivalent atoms. In this paper we combine the imaginary time/frequency approach of the STM with a novel representation of the response functions, based on localized Wannier-like orbitals, thus enhancing the scope of MBPT calculations so as to embrace systems potentially as large as a few hundreds atoms.

In the STM, the self-energy expectation value in Eq. (2) is obtained by analytically continuing to the real frequency axis the Fourier transform of the expression:

$$\langle \Sigma_{G^\circ W^\circ}(i\tau) \rangle_n = \mp \sum_l e^{\epsilon_l \tau} \times \int \psi_n(\mathbf{r}) \psi_l(\mathbf{r}) \psi_l(\mathbf{r}') \psi_n(\mathbf{r}') W(\mathbf{r}, \mathbf{r}'; i\tau) d\mathbf{r} d\mathbf{r}', \quad (3)$$

where the upper (lower) sign holds for positive (negative) times, the sum extends below (above) the Fermi energy, and QPAs are assumed to be real. By substituting  $v$  for  $W$ , Eq. (3) yields the exchange self-energy, whereas  $v \cdot \Pi \cdot v$  yields the correlation contribution,  $\Sigma_C$ , whose evaluation is the main size-limiting step of GW calculations.

Suppose that a small, time-independent, basis set to represent the polarizability exists:  $\Pi(\mathbf{r}, \mathbf{r}', i\tau) \approx \sum_{\mu\nu} \Pi_{\mu\nu}(i\tau) \bar{\Phi}_\mu(\mathbf{r}) \bar{\Phi}_\nu(\mathbf{r}')$ . Eq. (3) then gives:

$$\langle \Sigma_C(i\tau) \rangle_n \approx \mp \sum_{l\mu\nu} e^{\epsilon_l \tau} \Pi_{\mu\nu}(i\tau) S_{nl,\mu} S_{nl,\nu} \theta(E_C^1 - \epsilon_l), \quad (4)$$

where  $S_{nl,\nu} = \int \psi_n(\mathbf{r}) \psi_l(\mathbf{r}) \frac{1}{|\mathbf{r} - \mathbf{r}'|} \bar{\Phi}_\nu(\mathbf{r}') d\mathbf{r} d\mathbf{r}'$  and  $E_C^1$  is an energy cutoff that limits the number of conduction states to be used in the calculation of the self-energy. A convenient representation of the polarizability would thus allow QPEs to be calculated from Eq. (2), by analytically

continuing to the real axis the Fourier transform of Eq. (4). Such an optimal representation is identified in three steps: *i*) we first express the Kohn-Sham orbitals, whose products enter the definition of  $P^\circ$ , in terms of localized, Wannier-like, orbitals; *ii*) we then construct a basis set of localized functions for the manifold spanned by products of Wannier orbitals; finally, *iii*) this basis is further restricted to the set of eigenvectors of  $P^\circ$ , corresponding to eigenvalues larger than a given threshold.

Let us start from the RPA irreducible polarizability:

$$\tilde{P}^\circ(\mathbf{r}, \mathbf{r}'; i\omega) = \sum_{cv} \Phi_{cv}(\mathbf{r}) \Phi_{cv}(\mathbf{r}') \tilde{\chi}_{cv}^\circ(i\omega), \quad (5)$$

where  $\tilde{\chi}_{cv}^\circ(i\omega) = 2\text{Re} \left( \frac{1}{i\omega - \epsilon_c + \epsilon_v} \right)$  and  $\Phi_{cv}(\mathbf{r}) = \psi_c(\mathbf{r}) \psi_v(\mathbf{r})$ . We express valence and conduction QPAs in terms of localized, Wannier-like, orbitals:

$$\begin{aligned} u_s(\mathbf{r}) &= \sum_v \mathcal{U}_{sv}^{-1} \psi_v(\mathbf{r}) \theta(-\epsilon_v) \\ v_s(\mathbf{r}) &= \sum_c \mathcal{V}_{sc}^{-1} \psi_c(\mathbf{r}) \theta(\epsilon_c) \theta(E_C^2 - \epsilon_c), \end{aligned} \quad (6)$$

where  $E_C^2 \leq E_C^1$  is a second energy cutoff that limits a *lower conduction manifold* (LCM) to be used in the construction of the polarization basis. According to the choice of the  $\mathcal{U}$  and  $\mathcal{V}$  matrices, the  $u$ 's and  $v$ 's can be either maximally localized [7, 9] or non-orthogonal generalized [13] Wannier functions. We then reduce the number of product functions from the product between the number of valence and conduction states, which scales quadratically with the system size, to a number that scales linearly. To this end, we express the  $\Phi$ 's as approximate linear combinations of products of the  $u$ 's  $v$ 's:  $\Phi_{cv}(\mathbf{r}) \approx \sum_{rs} \mathcal{O}_{cv,rs} W_{rs}(\mathbf{r}) \theta(|W_{rs}|^2 - s_1)$ , where  $\mathcal{O}_{cv,c'v'} = \mathcal{U}_{vv'} \mathcal{V}_{cc'}$ ,  $W_{rs}(\mathbf{r}) = u_r(\mathbf{r}) v_s(\mathbf{r})$ ,  $|W_{cv}|$  is the  $L^2$  norm of  $W_{rs}(\mathbf{r})$ , which is arbitrarily small when the centers of the  $u_r$  and  $v_s$  functions are sufficiently distant, and  $s_1$  is an appropriate cutoff. The number of products can be further reduced on account of the non-orthogonality and mutual linear dependence of the  $W$ 's. To this end, let us define the overlap matrix:  $\mathcal{Q}_{\rho\sigma} = \int W_\rho(\mathbf{r}) W_\sigma(\mathbf{r}) d\mathbf{r}$ , where the  $\rho$  and  $\sigma$  indices stand for pairs of  $rs$  indices. The magnitude of the eigenvalues is a measure of linear dependence, and an orthonormal basis can be obtained by retaining only those eigenvectors  $\mathcal{U}_\nu$  whose eigenvalue,  $q_\nu$ , is larger than a given threshold,  $s_2$ :  $\bar{\Phi}_\nu(\mathbf{r}) \approx \frac{1}{\sqrt{q_\nu}} \sum_\rho \mathcal{U}_{\nu\rho} W_\rho(\mathbf{r})$ , for  $q_\nu > s_2$ . A final (and practically ultimate) refinement can be achieved by diagonalizing  $P^\circ$  in the basis thus reduced and by retaining only those eigenvectors whose eigenvalue is larger than a third threshold,  $s_3$ . The result of this last procedure would depend on frequency, which would make it impractical. We have verified, however, that the manifold spanned by the most important eigenvectors of  $P^\circ$  in the (imaginary) time domain depends very little on

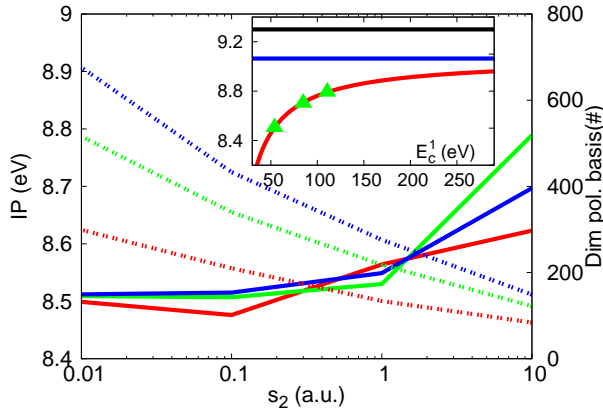


FIG. 1: Calculated ionization potential of the benzene molecule (solid lines, left scale) and dimension of the polarization basis (dashed lines, right scale) versus the  $s_2$  cutoff. The polarization basis has been constructed with a conduction energy cutoff  $E_C^2 = 16.7$  eV (red, 100 states),  $E_C^2 = 28.6$  eV (green, 300 states), and  $E_C^2 = 38.3$  eV (blue, 500 states). Inset: calculated ionization potential as a function of the overall conduction energy cutoff,  $E_C^1$ . Black line: experimental value; red line: fit to the calculated values (green triangles); blue line extrapolated value. See text for more details.

time, which permits the use of a same basis at different frequencies. When the basis for  $P^\circ$  is built out of *orthonormal* Wannier orbitals, this last refinement does not result in any further improvement if  $s_3 \geq s_2$  [14].

Once an optimal basis set has been thus identified, an explicit representation for the irreducible polarizability,

$$\tilde{P}^\circ(\mathbf{r}, \mathbf{r}, i\omega) = \sum_{\mu\nu} \tilde{P}_{\mu\nu}^\circ(i\omega) \overline{\Phi}_\mu(\mathbf{r}) \overline{\Phi}_\nu(\mathbf{r}'), \quad (7)$$

is obtained. By equating Eq. (5) to Eq. (7) and taking into account the orthonormality of the  $\overline{\Phi}$ 's, one obtains:

$$P_{\nu\mu}^\circ(i\omega) = \sum_{cv} T_{cv,\mu} T_{cv,\nu} \tilde{\chi}_{cv}^\circ(i\omega) \theta(E_C^1 - \epsilon_c), \quad (8)$$

where  $T_{cv,\mu} = \int \Phi_{cv}(\mathbf{r}) \overline{\Phi}_\mu(\mathbf{r}) d\mathbf{r}$ . A representation for  $\Pi$  is finally obtained by simple matrix manipulations.

Our scheme has been implemented in the QUANTUM ESPRESSO density functional package [15], for norm-conserving as well as ultra-soft pseudopotentials, resulting in a new module called *gww.x* which uses a Gauss-Legendre discretization of the imaginary time/frequencies half-axes, and that is parallelized accordingly. We first illustrate our scheme by considering an isolated benzene molecule in a periodically repeated cubic cell with an edge of 20 a.u. using a first conduction energy cutoff  $E_C^1 = 56.7$  eV, corresponding to 1000 conduction states, and a cutoff on the norm of Wannier products  $s_1 = 0.1$  a.u. [16]. In Fig. 1 we display the dependence of the calculated ionization potential (IP) on the second conduction energy cutoff used to define the

	Th1	Th2	prev th	Expt
$N_P$	4847	6510		
$\Gamma_{1v}$	-11.45	-11.49	-11.57	$-12.5 \pm 0.6$
$X_{1v}$	-7.56	-7.58	-7.67	
$X_{4v}$	-2.79	-2.80	-2.80	$-2.9, -3.3 \pm 0.2$
$\Gamma'_{25c}$	0.	0.	0.	0.
$X_{1c}$	1.39	1.41	1.34	1.25
$\Gamma'_{15c}$	3.22	3.24	3.24	$3.40, 3.05$
$\Gamma'_{2c}$	3.87	3.89	3.94	$4.23, 4.1$

TABLE I: QPEs (eV) calculated in crystalline silicon and compared with experimental (as quoted in Ref. 12) and previous theoretical results [12]. ‘Th1’ and ‘Th2’ indicate calculations made with  $s_2 = 0.01$  and  $s_2 = 0.001$  a.u. respectively, while  $N_P$  is the dimension of the polarization basis.

polarization basis,  $E_C^2$ , and on the cutoff on the eigenvalues of the overlap matrix between Wannier products,  $s_2$ . Convergence within 0.01 eV is achieved with a conduction energy cutoff  $E_C^2$  smaller than 30 eV (less than 300 states) and a polarization basis set of only  $\sim 400$  elements. The convergence of other QPEs is similar. The inset of Fig. 1, shows the convergence of the IP with respect to  $E_C^1$ , which turns out to be unexpectedly slow. These data can be accurately fitted by the simple formula  $IP(E_C^1) = IP(\infty) + A/E_C^1$ , resulting in a predicted ionization potential  $IP(\infty) = 9.1$  eV, in good agreement with the experimental value of 9.3 eV [17]. The potential of our method for large molecular system is illustrated by a calculation for the TPPH<sub>2</sub> molecule (C<sub>44</sub>H<sub>30</sub>N<sub>4</sub>) in a periodically repeated orthorhombic supercell of 75.6  $\times$  75.6  $\times$  26.5 a. u. [16]. Using values of 31.1, 40.5 and 48.1 eV for  $E_C^1$  (corresponding to 2000, 3000 and 4000 conduction states) and  $E_C^2 = 17.2$  eV (corresponding to 750 conduction states),  $s_1 = 1.5$  and  $s_2 = 0.01$  a.u., which lead to a basis of 2797 elements, yields an extrapolated  $IP(\infty)$  of 6.0 eV, in fair agreement with the experimental value of 6.4 eV [18].

In order to demonstrate our scheme for extended systems [19], we consider crystalline silicon treated using a 64-atom simple cubic cell [16] at the experimental lattice constant and sampling the corresponding Brillouin zone (BZ) using the  $\Gamma$  point only. This gives the same sampling of the electronic states as would result from 6 points in the irreducible wedge of the BZ of the elementary 2-atom unit cell. Our calculations were performed using  $E_C^1 = 94.6$  eV (corresponding to 3200 conduction states) and  $E_C^2 = 33.8$  eV (corresponding to 800 states in the LCM),  $s_1 = 1.0$  a.u. and two distinct values for  $s_2$  (0.01 and 0.001). In Tab. I we summarize our results and compare them with previous theoretical results, as well as with experiments. An overall convergence within a few tens meV is achieved with a  $s_2$  cutoff of 0.001 a.u., corresponding to a polarization basis of  $\sim 6500$  elements. The residual small discrepancy with respect to previous

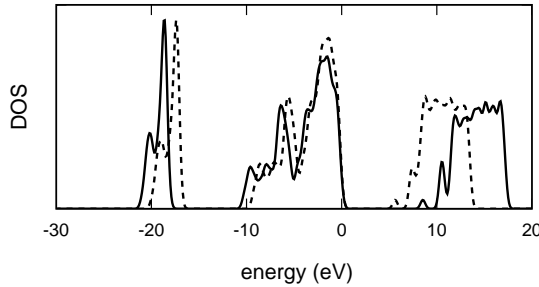


FIG. 2: Electronic density of states for a model of vitreous silica: LDA (dashed line) and GW (solid line). A Gaussian broadening of 0.25 eV has been used.

results [12] is likely due to our use of a supercell, rather than the more accurate k-point sampling used in previous work. Our ability to treat large supercells give us the possibility to deal with disordered systems that could hardly be addressed using conventional approaches. In Fig. 2 we show the QPE density of states as calculated for a 72-atom model of vitreous silica [16, 20]. We used  $E_C^1 = 48.8$  eV (corresponding to 1000 conduction states),  $E_C^2 = 30.2$  eV (corresponding to 500 states in the LCM),  $s_1 = 1$  a.u. and  $s_2 = 0.1$  a.u. (giving rise to a polarization basis of 3152 elements). We checked the convergence with respect to the polarization basis by considering  $s_2 = 0.01$  a.u. which leads to a basis of 3933 elements. Indeed, the calculated QPEs differ in average by only 0.01, eV with a maximum discrepancy of 0.07 eV [21]. The quasi-particle band-gap resulting from our calculations is 8.5 eV, to be compared with an experimental value of  $\sim 9$  eV [22] and with a significantly lower value predicted by DFT in the local-density approximation (5.6 eV).

In conclusion, we believe that expressing density response functions in terms of localized basis sets will permit to extend the scope of many-body perturbation theory to large models of molecular and extended, possibly disordered, systems. The extension of the methodology presented in this paper for quasi-particle spectra to optical spectroscopies using the Bethe-Salpeter formalism is straightforward and presently under way.

We thank C. Cavazzoni for his help in the parallelization of the code. This work has been partially funded under the Italian CNR-INFM *Seed Projects* scheme.

- [1] See *e.g.* R.M. Martin, *Electronic Structure* (Cambridge University Press, Cambridge, 2004) and references quoted therein.
- [2] L. Hedin and S. Lundqvist, *Solid State Phys.* **23**, 1 (1969).
- [3] F. Aryasetiawan and O. Gunnarsson, *Rep. Prog. Phys.* **61**, 237 (1998).
- [4] L. Hedin, *Phys. Rev.* **139**, 796 (1965).
- [5] M.S. Hybertsen and S.G. Louie, *Phys. Rev. Lett.* **55**, 1418 (1985).
- [6] G. Onida, L. Reining, and A. Rubio, *Rev. Mod. Phys.* **74**, 601 (2001).
- [7] N. Marzari and D. Vanderbilt, *Phys. Rev. B* **56**, 12847 (1997).
- [8] I. Souza, N. Marzari, and D. Vanderbilt, *Phys. Rev. B* **65**, 035109 (2001).
- [9] F. Gygi, J.-L. Fattebert, and E. Schwegler, *Comp. Phys. Comm.* **155**, 1 (2003).
- [10] S. Albrecht, L. Reining, R. Del Sole and G. Onida, *Phys. Rev. Lett.* **80**, 4510 (1998); M. Rohlfing and S.G. Louie, *Phys. Rev. B* **62**, 4927 (2000); L.X. Benedict, E.L. Shirley, and R.B. Bohn, *Phys. Rev. Lett.* **80**, 4514 (1998).
- [11] R. Shaltaf, G.-M. Rignanese, X. Gonze, F. Giustino, and A. Pasquarello, *Phys. Rev. Lett.* **100**, 186401 (2008).
- [12] H.N. Rojas, R.W. Godby, and R.J. Needs, *Phys. Rev. Lett.* **74**, 1827 (1995); M.M. Rieger, L. Steinbeck, I.D. White, H.N. Rojas, and R.W. Godby, *Comp. Phys. Comm.* **117**, 211 (1999).
- [13] F.A. Reboredo and A.J. Williamson, *Phys. Rev. B* **71**, 121105 (2005).
- [14] X.-F. Qian, private communication (2008).
- [15] P. Giannozzi et al., <http://www.quantum-espresso.org>.
- [16] DFT calculations were performed using the energy functional from J.P. Perdew and A. Zunger, *Phys. Rev. B* **23**, 5048 (1981) ( $C_6H_6$ , Si and  $SiO_2$ ) and that from J.P. Perdew, K. Burke, and M. Ernzerhof, *Phys. Rev. Lett.* **77**, 3865 (1996) ( $TTPH_2$ ). Pseudo-potentials have been taken from the Quantum ESPRESSO tables [15]. Norm-conserving: C.pz-vbc and H.pz-vbc for  $C_6H_6$ , Si.pz-rrkj for Si, Si.pz-vbc for  $SiO_2$ . Ultrasoft: O.pz-rrkjus for  $SiO_2$ , C.pbe-rrkjus, H.pbe-rrkjus and N.pbe-rrkjus for  $TTPH_2$ . The plane-wave cutoffs are as follows:  $C_6H_6$ : 40 (wavefunctions) and 160 Ry (density); Si: 18 and 72 Ry;  $SiO_2$ : 24 and 200 Ry;  $TTPH_2$ : 24 and 200 Ry.  $G^0W^0A$  calculations were performed using an imaginary time cutoff of 10 a. u. (20 a. u. for  $TTPH_2$ ), an imaginary frequency cutoff of 20 Ry (40 Ry for  $TTPH_2$ ), grids of 80 steps (320 for  $TTPH_2$ ); a two poles formula was used for fitting the self-energy [12].
- [17] N.O. Lipari, C.B. Duke, and L. Pietronero, *J. Chem. Phys.* **65**, 1165 (1976).
- [18] N.E. Gruhn, D.L. Lichtenberger, H. Ogura, and F.A. Walker, *Inor. Chem.* **38**, 4023 (1999).
- [19] The calculation of the screened interaction in infinite systems requires some further care. Because of the long-range character of the Coulomb interaction, accurate sampling of the BZ is needed to compute the long-wavelength components of the dielectric matrix [see S. Baroni and R. Resta, *Phys. Rev. B* **33**, 7017 (1986)]. In the present application to crystalline silicon, the ‘head’ ( $\mathbf{G} = \mathbf{G}' = 0$ ) and ‘wing’ ( $\mathbf{G} = 0, \mathbf{G}' \neq 0$ ) components of the dielectric matrix have been computed separately using a  $4 \times 4 \times 4$  grid for sampling the BZ of the 64-atom cubic cell, using density-functional perturbation theory. A  $2 \times 2 \times 2$  grid has been used to calculate the long-range contributions to the self-energy.
- [20] J. Sarnthein, A. Pasquarello, and R. Car, *Phys. Rev. Lett.* **74**, 4682 (1995); *Phys. Rev. B* **52**, 12 690 (1995).
- [21] The localization of Wannier orbitals permits to reduce the number of products required to calculate the  $S$  and  $T$  matrices by more than one order of magnitude with a loss of accuracy of 0.2-0.4 eV for the QPEs.

[22] F.J. Himpel, *Surf. Sci.* **168** 764, (1986); F.J. Grunthaner and P.J. Grunthaner, *Mater. Sci. Rep.* **1**, 65 (1986).